Journal of Molecular Catalysis A: Chemical 325 (2010) 1–7

Contents lists available at ScienceDirect

Journal of Molecular Catalysis A: Chemical

journal homepage: www.elsevier.com/locate/molcata

Editors Choice Paper

Hydrotreating activities of alumina-supported bimetallic catalysts derived from noble metal containing molecular sulfide clusters Mo_3S_4M' (M′ = Ru, Rh, Ir, Pd, Pt)

Konrad Herbst*, Michael Brorson, Anna Carlsson

Haldor Topsøe A/S, Nymøllevej 55, DK-2800 Lyngby, Denmark

ARTICLE INFO

Article history:
Received 8 January 2010
Received in revised form 23 March 2010
Accepted 24 March 2010
Available online 31 March 2010

Keywords:
Hydrotreating
Bimetallic catalyst
Noble metal
Sulfide cluster

ABSTRACT

Molecular sulfide clusters with bimetallic Mo_3S_4M' cluster cores (M′ = Ru, Rh, Ir, Pd, Pt) were impregnated on γ-alumina as the compounds $[(Cp')_3Mo_3S_4M'(L)_x][pts]_y$ (Cp′ = methylcyclopentadienyl; L = ligand; pts = *para*-toluenesulfonate). These catalyst precursors were sulfided at 350 °C leading to decomposition of the molecular clusters and the formation of MoS_2-like phases with optimal chances for noble metal atoms to be in close contact with MoS_2. The hydrotreating activities of the catalysts obtained were measured by using a feed containing dibenzothiophene, indole and naphthalene. The HDS, HDN and HYD activities followed the order $Mo_3Ir > Mo_3Rh > Mo_3Ru > Mo_3Pt > Mo_3Pd$. Comparison with the sum of activities of a monometallic Mo and a monometallic noble metal reference catalyst revealed strong synergies for the Mo_3Ir and Mo_3Rh catalysts, whose HDS and HDN activities had increased by factors of 2.7–3.9 and 1.8–4.3, respectively. A comparison with the hydrotreating activities of a Mo_3Ni catalyst prepared from $[(Cp')_3Mo_3S_4NiL][pts]$ showed, however, that the performances of the Mo_3Rh and Mo_3Ir catalysts generally were inferior by a factor of 2 to a Mo_3Ni catalyst. An inhibiting effect on the catalyst activity was observed for the Mo_3Pd catalyst. The sulfided Mo_3Rh, Mo_3Ir and Mo_3Pd catalysts were studied by TEM. The Mo_3Rh and Mo_3Ir catalysts showed a homogeneous and very high dispersion of both metals, the MoS_2 dispersion being higher than in the monometallic Mo reference catalyst. The Mo_3Pd catalyst showed a strong inhomogeneity due to the presence of 10 nm large Pd_4S particles fully encapsulated by layers of MoS_2.

1. Introduction

The industrially established catalysts for hydrotreating of oil at refineries are bimetallic sulfidic CoMo or NiMo phases supported on high surface area alumina [1]. The hydrotreating process serves several purposes in the upgrading of oil; most important are the removal of sulfur (hydrodesulfurization, HDS) and nitrogen (hydrodenitrogenation, HDN) from heterocyclic hydrocarbon molecules and the hydrogenation (HYD) of aromatic hydrocarbons.

In order to obtain fundamental understanding of the hydrotreating process and its catalysts, unsupported transition metal sulfides have been studied extensively both experimentally [2–8] and theoretically [9–13] for their HDS, HDN and HYD properties. The HDS activity of unsupported transition metal sulfides was correlated to the position of the metal in the periodic table [2] and later to the heats of formation of the transition metal sulfides [3]. In both cases characteristic volcano-type dependencies for the activities of 4d and 5d metal sulfides were observed. Later, a correlation was found between the HDS activity and the metal–sulfur bond energy covering both 3d, 4d and 5d transition metals [10,11]. All these studies agree that amongst the monometallic transition metal sulfides, the *noble metal* sulfides such as e.g. RuS_2 are found to be the most active HDS catalysts. Thus unsupported noble metal sulfide catalysts are typically one order of magnitude more active than an unsupported MoS_2 catalyst. However, MoS_2 gains substantial extra activity by promotion with cobalt or nickel and by dispersion on a high surface area support such as alumina. This, together with the relatively low metal prices, is the reason why CoMo and NiMo systems (atomic ratios Mo/Co = Mo/Ni ≈ 3) are preferred industrially.

The promotion of MoS_2-based alumina-supported catalysts by noble metals, rather than by Co or Ni, has also been the subject of several studies. In one such study it was found that the activities in dibenzothiophene HDS of a series of catalysts supported on amorphous silica–alumina ranked as PtMo > RuMo > PdMo > Mo [14]. This order of activity was confirmed by Meriño et al. for alumina-supported noble metal-molybdenum catalysts irrespective of the sulfidation procedure [15]. The same series of catalysts was also investigated in simultaneous HDS and HYD studies [16]. Furthermore, in a series of investigations by Vít and coworkers [17–21], iridium has been established as a strong promoter element for the HDN activity. Recently, these studies have been reviewed

* Corresponding author. Tel.: +45 4527 2678; fax: +45 4527 2999.
E-mail address: knh@topsoe.dk (K. Herbst).

1381-1169/$ – see front matter © 2010 Elsevier B.V. All rights reserved.
doi:10.1016/j.molcata.2010.03.031

[22] and the investigations have also been extended to other noble metals [23–25]. The sulfidation mechanism and HDS/HDN activities of alumina or zeolite supported noble metal catalysts have also been investigated by Paál et al. [26,27] and Prins and coworkers [28,29].

In preparing a promoted catalyst it is essential that the preparative procedure results in the promoter atoms being present in close contact with the structures that are to be promoted. In the investigations of noble metal-molybdenum catalysts mentioned above, the catalysts were typically prepared by sequential impregnation or co-impregnation of the relevant metals in aqueous solutions. However, in order to optimize the chances for Mo and a potential promoter metal being intimately mixed in the final catalyst, molecular heterobimetallic sulfide clusters containing cubane-like Mo_3S_4M' (M′ = Co, Ni, other metals) cores constitute a very interesting opportunity [30]. Not only do the clusters contain the desired metal atoms in the correct ratio within one single molecular species, they are also sulfidic and the molybdenum is pre-reduced to the oxidation state +4. These Mo_3S_4M' (M′ = Co, Ni) clusters have been investigated as structural models [31,32] for the active centres of industrial CoMo and NiMo hydrotreating catalysts and as potential homogeneous HDS catalysts in the liquid phase [31,33–36]. As precursor for supported catalysts, only the $Mo_3S_4Ni^{4+}$ cluster has previously been used in studies, where the aqua complex $[(H_2O)_9Mo_3S_4Ni(Cl)]^{4+}$ was incorporated by ion-exchange into various zeolites [37,38]. The deposition of nickel or cobalt salts of related $[Mo_3S_{13}]^{2-}$ clusters onto alumina has been investigated by Fedin et al. [39].

We have previously extended the series of available cubane-like Mo_3S_4M' clusters by the insertion of noble metals complexes into Mo_3S_4 clusters stabilized by methylcyclopentadienyl ligands [40,41]. With the extensive series of clusters with Mo_3S_4M' cores (M′ = Ru, Rh, Ir, Pd, Pt) now available as precursor compounds, we here report a systematic study of the promotional influence of noble metals on alumina-supported MoS_2-based catalysts derived from Mo_3S_4M' clusters.

2. Experimental

2.1. Catalyst precursor preparation

The bimetallic cluster compounds $[(\eta^5\text{-Cp}')_3Mo_3S_4Ru(CO)_2][pts]$ [41], $[(\eta^5\text{-Cp}')_3Mo_3S_4Rh(cod)][pts]_2$ [41], $[(\eta^5\text{-Cp}')_3Mo_3S_4IrCl(cyclooctene)][pts]$ [41], $[(\eta^5\text{-Cp}')_3Mo_3S_4Pd(PPh_3)][pts]$ [40] and $[(\eta^5\text{-Cp}')_3Mo_3S_4Pt(norbornene)][pts]$ [40] were prepared according to published procedures (Cp′ = methylcyclopentadienyl; cod = 1,5-cyclooctadiene; pts = *p*-toluenesulfonate). CH_2Cl_2 solutions of the clusters were impregnated on γ-alumina (BET area ≈300 m^2/g, 600–850 μm granules, predried at 150 °C for 2 h) by incipient wetness impregnation. Subsequently, the catalyst precursors were dried in a vacuum at ambient temperature.

Monometallic reference catalysts were prepared by impregnation with CH_2Cl_2 solutions of $M(acac)_3$ (M = Ru, Rh, Ir; acac = acetylacetonate; Aldrich), $M(acac)_2$ (M = Pd, Pt; Aldrich) or $[(\eta^5\text{-Cp}')_3Mo_3S_4][pts]$ [40] on alumina granules and subsequent drying in vacuum at ambient temperature.

For the analysis of the metal loads, a part of each sample was dried at 250 °C, and analyzed by Inductively Coupled Plasma Spectroscopy (ICP). The metal loads, both for freshly impregnated catalysts and for spent sulfided catalysts, are shown in Table 1.

2.2. Catalytic activity measurements

The activity measurements were made in a tubular 7.5 mm inner diameter, high-pressure flow reactor loaded with a mixture of 0.30 g catalyst and glass microbeads. Upon entry into the hot reactor the liquid feed was evaporated and mixed with a stream of H_2. *In situ* sulfidation was made for 4 h at 350 °C by means of a 2.5% solution of dimethyldisulfide (DMDS) in *n*-heptane and with $p(H_2) = 42$ atm. The feed for the activity measurements was an *n*-heptane solution containing 3.0% dibenzothiophene, 0.5% indole, 1.0% naphthalene, 2.5% dimethyldisulfide and 0.5% *n*-nonane (internal GC standard). The total pressure (reactants + *n*-heptane + H_2) at the reactor temperature of 350 °C was 50 atm corresponding to $p(H_2) = 38$ atm. Liquid feed to gaseous H_2 ratio was 0.5 ml/min:250 Nml/min. The partial pressure of H_2S from HDS of DMDS ensures that catalysts remain fully sulfided during the catalytic tests.

During the ≈24 h catalytic test, the composition of the exit gas from the reactor was continuously quantified by GC-FID (column: non-polar WCOT, Hewlett-Packard Ultra 2). Under the reaction conditions employed, dibenzothiophene (DBT) was desulfurized by two parallel routes yielding either biphenyl (bp) or cyclohexylbenzene (chb) as products. Indole was denitrogenated to yield ethylbenzene and ethylcyclohexane as products. Naphtalene was hydrogenated to tetralene. The conversions determined were expressed as pseudo first order rate constants for hydrodesulfurization (HDS), hydrodenitrogenation (HDN) and hydrogenation (HYD), respectively. The rate constants were determined typically after 24 h reaction time, after the conversion rate had been at a constant level for at least 10 h.

2.3. Raman measurements

Raman spectroscopy was performed on a Labram I (Dilor) instrument equipped with a confocal microscope (Olympus). A notch filter was applied to cut off the laser-line and the Rayleigh scattering up to 150 cm^{-1}. The spectrometer is equipped with a CCD

Table 1
Chemical analysis data for the catalyst precursors impregnated on alumina and the spent sulfided catalysts.

Metals	Catalysts after impregnation and drying			Spent sulfided catalysts		
	wt% Mo	wt% M′	Atomic ratio Mo:M′	wt% Mo	wt% M′	Atomic ratio Mo:M′
Mo_3	8.57			8.51		
Mo_3S_4Ru	8.60	3.11	3:1.03	N/A	N/A	N/A
Mo_3S_4Rh	8.14	2.67	3:0.92	8.96	2.89	3:0.90
Mo_3S_4Ir	8.59	5.66	3:0.99	8.19	5.51	3:1.01
Mo_3S_4Pd	8.67	3.14	3:0.98	8.27	2.98	3:0.97
Mo_3S_4Pt	8.83	5.79	3:0.97	8.66	5.70	3:0.97
Ru		2.64			2.64	
Rh		2.68			2.60	
Ir		4.65			4.68	
Pd		2.59			2.64	
Pt		4.82			4.92	
Mo_3S_4Ni	12.9	2.45	3:0.93	N/A	N/A	N/A

camera (1024 × 298 diodes), which is Peltier cooled to 243 K to reduce the thermal noise. The 514 nm of an Ar-ion laser, with an approx. power of 2 mW at the sample, was used for excitation. The following spectrometer parameters were used: microscope objective: 100×, grating: 1800 g/mm, slit width: 300 μm, integration time: 600 s, accumulations: 5×. The Raman spectrum of the unsupported Mo_3S_4Ir cluster and the freshly impregnated catalyst were measured in air, whereas the spent catalyst was measured in an atmosphere of N_2.

2.4. TEM investigations

Fresh catalyst samples were sulfided in the activity test reactor for 4 h at 350 °C by means of a 2.5% solution of dimethyldisulfide (DMDS) in *n*-heptane and with $p(H_2) = 42$ atm. The samples were transferred to the microscope under inert conditions. The TEM (CM200 FEG from Philips/FEI) was coupled with electron-dispersive spectroscopy (EDS) mapping to determine the distribution of different elements in the samples.

3. Results and discussion

3.1. Catalytic measurements

The objective of the present study was to compare the hydrotreating activities of monometallic Mo and noble metal catalysts with the activities of bimetallic catalysts derived from molecular sulfide clusters containing molybdenum and a noble metal atom. The monometallic noble metal reference catalysts were prepared by impregnation of acetylacetonato metal complexes $M(acac)_2$ (M = Pd, Pt) or $M(acac)_3$ (M = Ru, Rh, Ir) on γ-alumina. The common feature in the series of heterobimetallic sulfide cluster compounds used in this study is the cubane-like cluster core Mo_3S_4M' (M′ = Ru, Rh, Ir, Pd, Pt), in which the catalytically relevant metals are in a sulfidic state and pre-assembled in a 3:1 atomic ratio at the molecular level. Methylcyclopentadienyl ligands are coordinated to the cluster Mo atoms and organic ligands (typically alkenes) are coordinated to the noble metal heteroatom. The structures of the cluster compounds are shown in Scheme 1. Concentrated solutions of the cluster compounds in CH_2Cl_2 were used for impregnation on γ-alumina. By using the same procedure, a monometallic Mo reference catalyst precursor was prepared from the cluster $[(\eta^5\text{-Cp}')_3Mo_3S_4][pts]$.

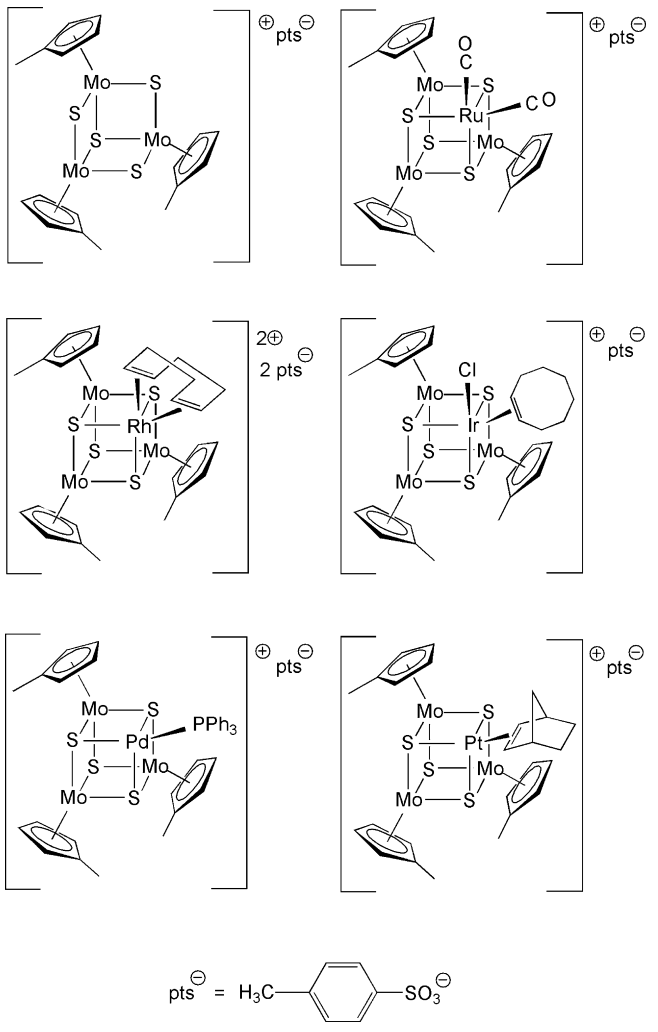

Scheme 1. Molecular formulae of the cluster compounds used for impregnation on alumina.

Raman spectra of the dried, cluster-impregnated catalyst precursors showed bands at the same wavenumbers as seen for the unsupported cluster compounds. Since also the linewidths of the signals are practically unchanged it can be concluded that the molecular clusters were intact after impregnation on the alumina carrier, where the clusters crystallized as a thin layer on the carrier surface. As an example, Fig. 1 shows the Raman spectra of the Mo_3Ir cluster as pure compound (trace (a)) and after impregnation/drying on alumina (trace (b)). By comparison with Raman data on Mo and Ir compounds published in the literature [42–44], some bands in traces (a) and (b) can tentatively be assigned to specific vibrations. A band at 222 cm^{-1} is indicative for Mo–Mo stretching vibrations, whereas a set of bands between 290 and 410 cm^{-1} is characteristic for M–S stretching vibrations (both Mo–S and Ir–S). Bands at 435 and 459 cm^{-1} can be assigned to Mo–C vibrations. The organic ligands (Cp′ and cyclooctene) display bands in the 830–860, 1225 and 1580 cm^{-1} regions.

All catalyst precursor samples were subjected to an *in situ* sulfidation procedure with dimethyl disulfide at 350 °C immediately before the actual activity measurements. Structural disintegration of the clusters takes place in the temperature range of 160–180 °C. The sulfidation at 350 °C thus removes the volatile organic ligands

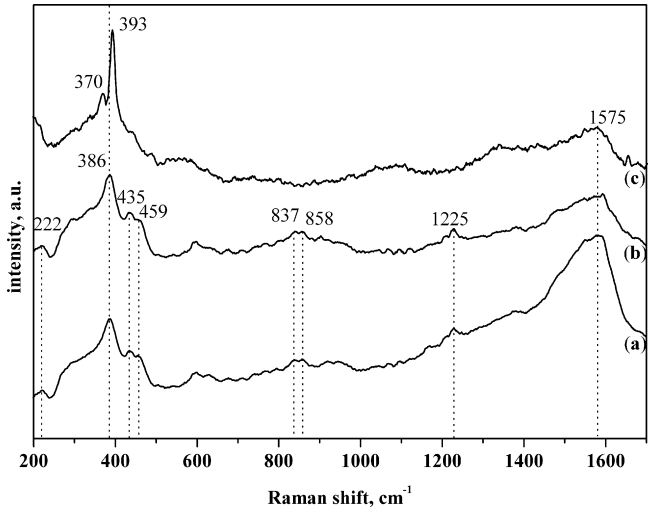

Fig. 1. Raman spectrum of $[(\eta^5\text{-Cp}')_3Mo_3S_4IrCl(cycloocten)][pts]$ and the fresh sulfided Mo_3Ir catalyst. Trace (a) bulk cluster compound. Trace (b) cluster impregnated on alumina and dried in vacuum. Trace (c) spent sulfided catalyst.

coordinated to the cluster cores and decomposes the cluster cores to MoS_2-like phases with noble metal atoms in close vicinity. This activation/sulfidation procedure ensures that the MoS_2-like catalysts are present on the carrier surface in their final sulfidic state before the hydrotreating activity measurements start. The Raman spectrum of the sulfidic phase is shown in Fig. 1 (trace (c)). The bands at 393 and 370 cm^{-1} clearly demonstrate that the cluster upon sulfidation has been converted to a MoS_2-like phase. MoS_2-derived bands around 400 and 370 cm^{-1} have previously been assigned to the $\nu(E^1_{2g})$ and $\nu(A_{1g})$ vibrations of MoS_2, respectively [45]. The broad band around 1575 cm^{-1} in trace (c) indicates the presence of carbonaceous compounds on the spent sulfided catalysts which originate from the catalytic tests.

The activities of the catalysts were measured on a model diesel feed containing dibenzothiophene, indole and naphthalene dissolved in *n*-heptane. These three compounds are representative for the sulfur, nitrogen and aromatic hydrocarbon compounds found in oil with a boiling point range corresponding to diesel. The raw activity data are listed in Table 2. Although the aim was to prepare catalysts and references with identical metal loads, the exact target load was not always obtained. Thus, *small* differences in the metal loads of the freshly prepared catalysts to be compared (see Table 1) have been corrected by normalization of the activity to the same metal content, 8.50 wt% Mo, corresponding to 0.266 mmol Mo on 300 mg catalyst material used for a catalytic test. Accordingly, the activities of the heterometal reference catalysts have been normalized to 0.266/3 = 0.089 mmol. Proportionality between metal load and first order rate constant was in other words assumed in a *narrow* interval around the experimentally determined metal load. A graphical representation of the normalized activities is given in Fig. 2, where all columns represent exactly the same molar amount of metal atoms and therefore can be compared directly. As basis for the activity calculations shown in Fig. 2, the metal contents of the freshly impregnated catalysts have been used.

The HDS activities of the monometallic catalysts follow the order Mo < Ru = Pd < Rh < Ir < Pt. Part of this trend has, when recalculated to a molar basis, previously been found in a study of Mo, Ru, Pd and Pt catalysts derived from noble metal chlorides impregnated on γ-alumina [15]. In our own previous study of the HDS activities of unsupported noble metal sulfides, where support effects from γ-alumina do not play a role, the activities followed the order Mo < Rh < Pd < Ru [7]. In the present study, HDN and HYD activities follow each other closely, with Ru and Rh as the least active catalysts. The Mo catalyst, which had only moderate activity in HDS, had the best performance in HDN and HYD.

The bimetallic catalysts showed the same order of activities for HDS, HDN and HYD, in all cases increasing in the order $Mo_3Pd < Mo_3Pt < Mo_3Ru < Mo_3Rh < Mo_3Ir$. The variation in HDS activity between the least active (Mo_3Pd) and the most active (Mo_3Ir) catalyst was almost one order of magnitude. For HDN, the activity variation was even more pronounced – the Mo_3Ir catalyst was 330 times more active than the Mo_3Pd catalyst.

We now turn to the issues of synergy and promotion. By comparing the sum of activities of the monometallic Mo and the monometallic noble metal catalysts with the activity of the cluster-derived bimetallic catalysts, it is seen that the Mo_3Ru catalyst has somewhat higher activities than the sum of the Mo_3 and Ru catalysts (see Fig. 2). Much more pronounced is the synergy for Mo_3Rh and Mo_3Ir. With regard to HDS, the activity of the Mo_3Rh catalyst is a factor of 3.9 times higher than the sum of the Mo_3 and Rh reference catalysts; for Mo_3Ir the corresponding factor is 2.7. Similarly pronounced synergies were found for HDN. While the HDN activities of the monometallic Rh and Ir reference catalysts were low, the bimetallic Mo_3Rh or Mo_3Ir catalysts showed synergies for HDN by factors of 1.8 and 4.3, respectively. At the other end of the scale, the presence of Pd and Pt had an inhibiting effect on the hydrotreating activities of a MoS_2 catalyst. Especially Pd, which amongst the noble metal catalysts performed the best with regard to both HDN and HYD, had a strong inhibiting effect on the HDS, HDN and HYD activities of a MoS_2 catalyst.

Co and Ni are, as mentioned above, established as strong promoters in MoS_2-based catalysts. In order to assess, on an absolute scale, the extent of promotion brought about by the noble metals in the Mo_3Rh and Mo_3Ir catalysts, a comparison can be made with a Mo_3Ni catalyst. This catalyst was previously prepared from the cluster $[(\eta^5\text{-}Cp')_3Mo_3S_4Ni(cyclooctadiene)][pts]$ by impregnation on γ-alumina and obtained higher metal loadings (12.9 wt% Mo, 2.45 wt% Ni) than the noble metal containing catalysts prepared for the current study. The sulfidation and activity test procedures for this Mo_3Ni catalyst were the same as used in the present study. After normalization to 0.089 mmol Mo_3Ni, the HDS activity of this catalyst is 1.9 and 1.7 times higher than the HDS activities of Mo_3Rh and Mo_3Ir catalysts, respectively. For HDN, the normalized activity of Mo_3Ni is 2.5 times higher than that of the Mo_3Rh catalyst while the HDN activities of Mo_3Ni and Mo_3Ir are on the same level. This shows that, although an impressive promotional effect of Rh and Ir on MoS_2 is observed, even the most active noble metal containing catalysts prepared from heterobimetallic cluster sources are generally inferior to the hydrotreating performance of a Mo_3Ni catalyst.

The hydrogenation activity of the catalysts of this study is directly measured in terms of their ability to catalyse hydrogenation of naphthalene, but is also reflected in the selectivity for formation of the two HDS products biphenyl (bp) and cyclohexylbenzene (chb). These selectivities are expressed in Table 2 as the ratio between chb and bp [46]. Bp is formed by direct desulfurization of dibenzothiophene, i.e. without hydrogenation, whereas chb is formed by hydrogenation of one benzo-ring preceding desulfurization. Both the monometallic and bimetallic catalysts had a relatively low selectivity towards chb (chb/bp ratio between 0

Table 2
Experimentally determined pseudo first order rate constants for HDS, HDN and HYD (bp = biphenyl; chb = cyclohexylbenzene).

Metals	k (HDS) [h^{-1}]	k (bp) [h^{-1}]	k (chb) [h^{-1}]	Ratio k (chb)/k (bp)	k (HDN) [h^{-1}]	k (HYD) [h^{-1}]
Mo_3	1.9	1.7	0.2	0.12	6.0	3.8
Mo_3S_4Ru	6.9	6.8	0.1	0.01	2.6	2.5
Mo_3S_4Rh	19.1	17.4	1.7	0.10	12.7	4.8
Mo_3S_4Ir	22.8	21.7	1.2	0.06	33.0	6.3
Mo_3S_4Pd	2.6	2.5	0.1	0.04	0.1	0.6
Mo_3S_4Pt	4.0	4.0	0.1	0.03	1.5	1.1
Ru	2.4	2.4	0	0	0.1	0.4
Rh	2.8	2.8	0	0	1.1	0.7
Ir	5.4	5.4	0	0	1.3	1.7
Pd	2.2	2.1	0.1	0.05	2.7	2.9
Pt	6.7	6.7	0	0	2.1	1.5
Mo_3S_4Ni	57.1	42.7	14.4	0.34	47.8	32.3

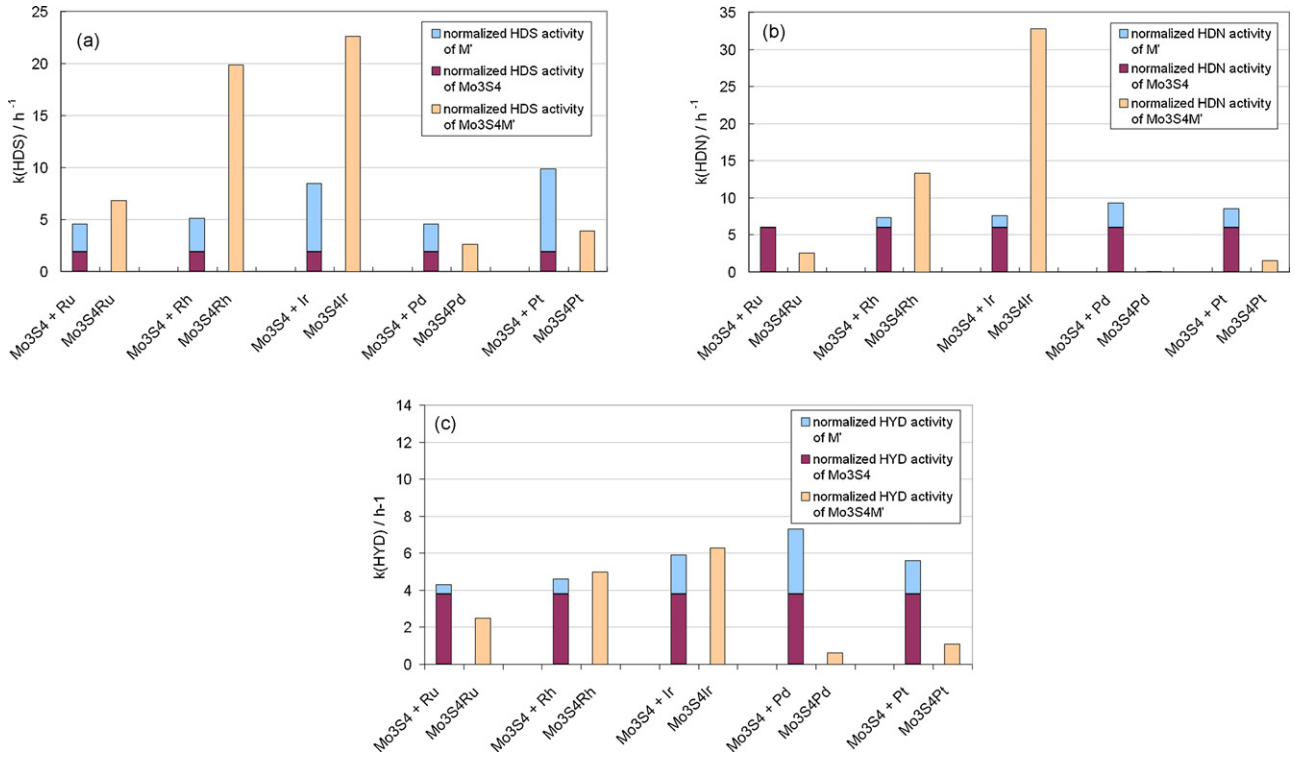

Fig. 2. (a)–(c) The sum of Mo_3S_4 and M′ activities compared to the relative Mo_3S_4M' activity. (a) HDS activities; (b) HDN activities; (c) HYD activities. The activities have been normalized to 0.266 mmol Mo and 0.089 mmol M′, so that each column represents the same number of metal atoms.

and 0.10) compared to $CoMo/Al_2O_3$ and $NiMo/Al_2O_3$ for which chb/bp ratios typically are 0.15 and 0.35, respectively, under identical reaction conditions. All the monometallic catalysts of this study, apart from the Pd catalyst, desulfurized DBT exclusively via the direct route. The chb/bp ratio for Mo catalysts is apparently strongly dependent on preparation conditions; for Mo catalysts prepared by impregnation with ammonium dimolybdate or ammonium heptamolybdate solutions, the ratio usually lies in the range of 0.20–0.25, whereas for the present Mo catalyst, the chb/bp ratio is 0.12.

Vít and coworkers have in a series of papers [17–25] been addressing the issue of noble metal promotion of MoS_2/Al_2O_3 hydrotreating catalysts. Direct comparisons with our results are not possible due to differences in the conditions for catalytic activity measurements and, in particular, in the metal loads of the catalysts and in the choice of sulfur and nitrogen compounds studied. Irrespective of this, we will, however, attempt to make some comparisons of a general nature. There is certainly agreement that Ir [21] and Rh [23] are the best promoters amongst the noble metals. Somewhat contrary to Vít and coworkers [23–25] we do not find that Pd, Pt and Ru have any substantial promotional effect. Specifically for Rh, Vít and coworkers find [19] that $RhMo/Al_2O_3$ is more active than CoMo and $NiMo/Al_2O_3$ catalysts for HDS of thiophene. For dibenzothiophene our results show that the ranking is reversed, i.e. RhMo is somewhat less active than $NiMo/Al_2O_3$. However, in both cases Rh displays a promotional effect of the same magnitude as that of the two industrial promoters. As far as Ir is concerned, there is consensus that Ir promotes HDN more than HDS in Mo/Al_2O_3 catalysts [17].

3.2. TEM investigations

The Mo_3 catalyst, the least active bimetallic catalyst (Mo_3Pd) and the two most active bimetallic catalysts (Mo_3Rh and Mo_3Ir), were all characterized by transmission electron microscopy (TEM) in order to investigate if the catalyst morphology may account for the large activity differences. Fresh catalyst samples were sulfided in the test reactor using the same sulfidation program as for the catalytic tests, and transferred to the microscope under inert conditions. Representative microscope images for the sulfided Mo_3, Mo_3Pd and Mo_3Ir catalysts are displayed as Figs. 3–5. A statistical evaluation of the MoS_2 slab length and the order of stacking for all catalysts investigated by TEM is given in Table 3.

The catalyst originating from the Mo_3 cluster shows a homogeneous dispersion of MoS_2 slabs (Fig. 3). A statistical evaluation of the MoS_2 slab size counted for ca. 500 particles (see Figs. 6 and 7)

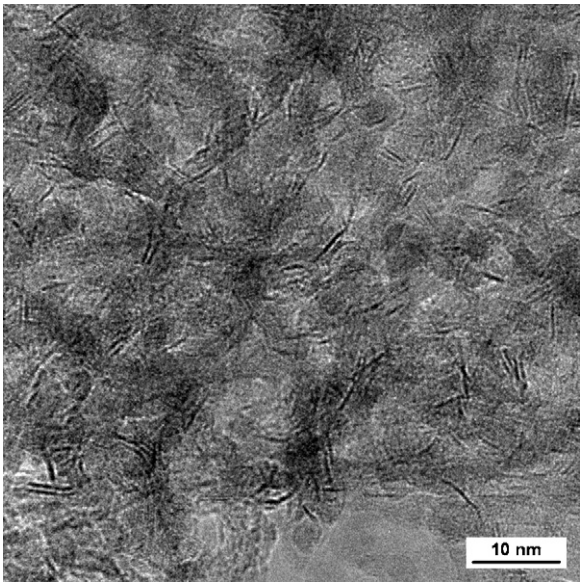

Fig. 3. TEM image of the MoS_2 catalyst derived from the Mo_3S_4 cluster.

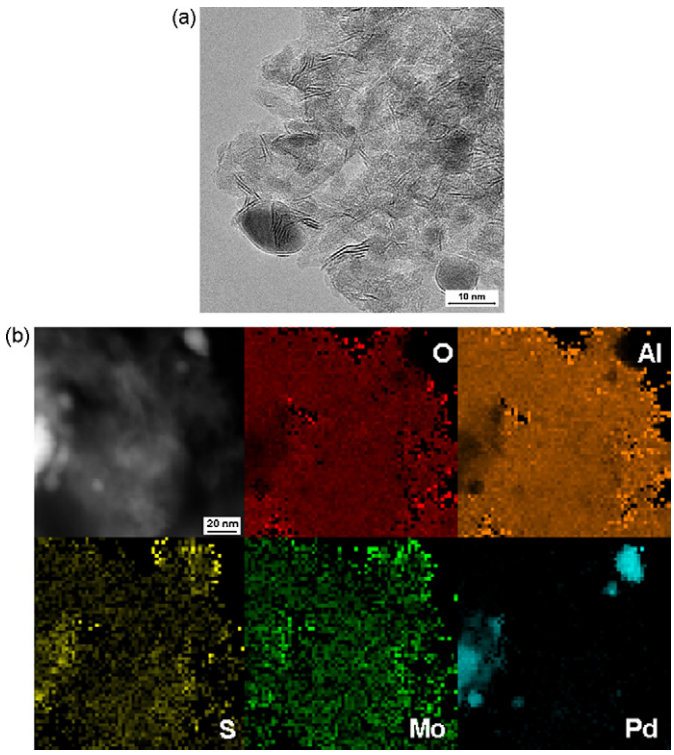

Fig. 4. (a) TEM image, (b) elemental map of the sulfided Mo_3Pd catalyst.

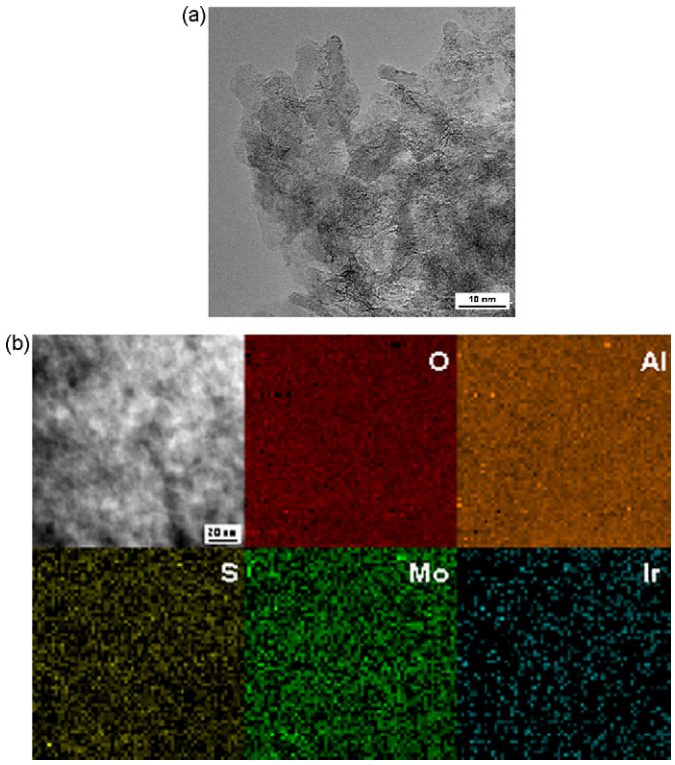

Fig. 5. (a) TEM image, (b) elemental map of the sulfided Mo_3Ir catalyst.

Table 3
Statistical evaluation of MoS_2 slab length and order of stacking.

Catalyst	Average length [nm]	Average number of slabs
Mo_3	2.69 (0.06)	2.08 (0.07)
Mo_3Pd	2.81 (0.07)	2.09 (0.06)
Mo_3Ir	2.10 (0.05)	1.24 (0.02)
Mo_3Rh	1.78 (0.05)	1.10 (0.01)

revealed an average slab length L_{av} of 2.69 (0.06) nm, which is similar to previous determinations of the slab length of conventionally prepared MoS_2/alumina catalysts [21,47,48]. The distribution of the number of slabs shows an average stacking order N_{av} of 2.08 (0.07), with ca. 50% of the MoS_2 particles present as single layer slabs and 30% as double layer slabs.

TEM characterization of the bimetallic catalysts revealed distinct differences in catalyst morphologies, which were reflected both in the TEM images and in the statistical evaluation of the MoS_2 particle size. TEM images of the catalyst originating from the Mo_3Pd cluster revealed a strong inhomogeneity of the catalyst (Fig. 4a). Palladium was present in large particles (10–15 nm) on the alumina surface, and these particles are at least partially encapsulated by MoS_2. Under the sulfidation conditions employed, the Pd atoms were obviously expelled from the Mo_3Pd cluster and sintered to large monometallic particles. From the elemental map (Fig. 4b), the MoS_2 shell around the large palladium particles can be detected as well. The nature of these palladium particles was revealed by XRPD analyses of the spent Mo_3Pd catalyst as well as the monometallic Pd reference catalyst, which detected Pd_4S as the only crystalline palladium phase. Also previous studies on the activities of noble metal-molybdenum catalysts have identified Pd_4S on sulfided samples [27]. The statistical analysis revealed that the distribution of length and stacking order of the MoS_2 slabs was approximately the same as for the Mo_3 reference catalyst (L_{av} = 2.81 nm, N_{av} = 2.09).

In sharp contrast to the inhomogeneous metal dispersion on the Mo_3Pd catalyst, the Mo_3Rh and Mo_3Ir catalysts showed much more homogeneous metal dispersions both for Mo and the noble metal (Fig. 5a and b for the Mo_3Ir catalyst). The MoS_2 slabs were almost exclusively present as monolayer slabs and were reduced

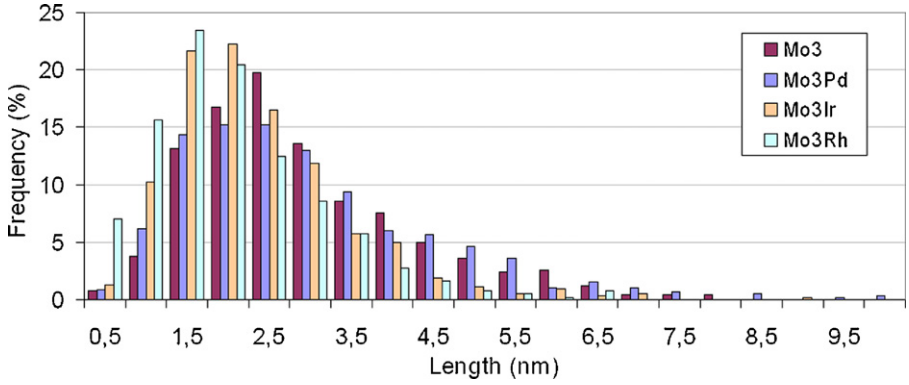

Fig. 6. Statistical distribution of MoS_2 slab lengths for the sulfided Mo_3, Mo_3Pd, Mo_3Ir and Mo_3Rh catalysts.

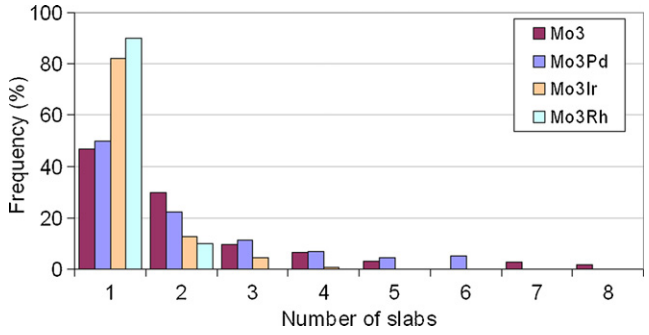

Fig. 7. Statistical distribution of number of slabs per MoS_2 particle for the sulfided Mo_3, Mo_3Pd, Mo_3Ir and Mo_3Rh catalysts.

in their average length to 2.10 nm (Mo_3Ir) and 1.78 nm (Mo_3Rh), respectively. Iridium and rhodium were present as particles so small (<2 nm), that they could hardly be visualized. A homogeneous distribution of Rh and Ir over the catalyst samples was found. In the case of Ir, this is seen in the elemental map of the Mo_3Ir catalyst (Fig. 5b). The 150 × 150 nm section scanned by EDS is virtually free of any local concentration maxima of Mo, Ir or S. From the present data (an XRPD analysis did not detect any Ir-containing phases due to the small particles size) it is difficult to decide whether iridium is present in metallic or sulfided state. However, the high H_2 partial pressure (38 bar) during the activation suggests that Ir could have been reduced to metal during the test.

4. Conclusions

The TEM characterization of the least active and most active bimetallic catalysts has shown that the promotional effect seen for Rh and Ir containing catalysts may at least in part be ascribed to a better distribution of the MoS_2 slabs on the alumina carrier. From the present data it is difficult to state if the noble metal is completely present as a separate phase beside the MoS_2 phase or if a part of the noble metal atoms are located in direct contact with the MoS_2 phase, forming an Ir–Mo–S or Rh–Mo–S structure similar to the known Co–Mo–S and Ni–Mo–S structures [49–51]. This question is of great importance for the activation of H_2 on the mixed noble metal/Mo catalysts, but requires additional characterization, e.g. by *in situ* EXAFS, and extended calculations.

Acknowledgements

The authors thank Peder Blom for conducting the catalytic experiments and Dr. Pablo Beato for his assistance in recording the Raman spectra.

References

[1] H. Topsøe, B.S. Clausen, F.E. Massoth, in: J.R. Anderson, M. Boudard (Eds.), Catalysis – Science and Technology, Springer, Berlin, 1996, p. 22ff.
[2] T.A. Pecoraro, R.R. Chianelli, J. Catal. 67 (1981) 430.
[3] R.R. Chianelli, Catal. Rev. Sci. Eng. 26 (1984) 361.
[4] A.P. Raje, S.-J. Liaw, R. Srinivasam, B.H. Davis, Appl. Catal. A: Gen. 150 (1997) 297.
[5] M. Cattenot, J.-L. Portefaix, J. Afonso, M. Breysse, M. Lacroix, G. Perot, J. Catal. 173 (1998) 366.
[6] M. Lacroix, N. Boutarfa, C. Guillard, M. Vrinat, M. Breysse, J. Catal. 120 (1989) 473.
[7] N. Herman, M. Brorson, H. Topsøe, Catal. Lett. 65 (2000) 169.
[8] A. Ishihara, F. Dumeignil, J. Lee, K. Mitsuhashi, E.W. Qian, T. Kabe, Appl. Catal. A: Gen. 289 (2005) 163.
[9] S. Harris, R.R. Chianelli, J. Catal. 86 (1984) 400.
[10] J.K. Nørskov, B.S. Clausen, H. Topsøe, Catal. Lett. 13 (1992) 1.
[11] H. Topsøe, B.S. Clausen, N.-Y. Topsøe, J. Hyldtoft, J.K. Nørskov, Am. Chem. Soc, Petrol Div. Prep. 38 (1993) 638.
[12] H. Toulhoat, P. Raybaud, S. Kasztelan, G. Kresse, J. Hafner, Catal. Today 50 (1999) 629.
[13] H. Toulhoat, P. Raybaud, J. Catal. 216 (2003) 63.
[14] R. Navarro, B. Pawelec, J.L.G. Fierro, P.T. Vasudevan, Appl. Catal. A: Gen. 148 (1996) 23.
[15] L.I. Meriño, A. Centeno, S.A. Giraldo, Appl. Catal. A: Gen. 197 (2000) 61.
[16] D. Pérez-Martínez, S.A. Giraldo, A. Centeno, Appl. Catal. A: Gen. 315 (2006) 35.
[17] J. Cinibulk, Z. Vít, Appl. Catal. A: Gen. 204 (2000) 107.
[18] Z. Vít, J. Cinibulk, React. Kinet. Catal. Lett. 72 (2001) 189.
[19] Z. Vít, J. Cinibulk, React. Kinet. Catal. Lett. 77 (2002) 43.
[20] J. Cinibulk, Z. Vít, Stud. Surf. Sci. Catal. 143 (2002) 443.
[21] J. Cinibulk, D. Gulková, Y. Yoshimura, Z. Vít, Appl. Catal. A: Gen. 255 (2003) 321.
[22] Z. Vít, Appl. Catal. A: Gen. 322 (2007) 142.
[23] Z. Vít, J. Cinibulk, D. Gulková, Appl. Catal. A: Gen. 272 (2004) 99.
[24] Z. Vít, D. Gulková, L. Kaluža, M. Zdražil, J. Catal. 232 (2005) 447.
[25] D. Gulková, Y. Yoshimura, Z. Vít, Appl. Catal. B: Environ. 87 (2009) 171.
[26] M. Dobrovolszky, K. Matusek, Z. Paál, P. Tétényi, J. Chem. Soc. Faraday Trans. 89 (1993) 3137.
[27] Z. Paál, T. Koltai, K. Matusek, J.-M. Mamoli, C. Potvin, M. Muhler, U. Wild, P. Tétényi, Phys. Chem. Chem. Phys. 3 (2001) 1535.
[28] Y. Sun, R. Prins, Angew. Chem. Int. Ed. 47 (2008) 8478.
[29] A. Niquille-Röthlisberger, R. Prins, J. Catal. 242 (2006) 207.
[30] M.D. Curtis, Appl. Organomet. Chem. 6 (1992) 429.
[31] K. Herbst, M. Monari, M. Brorson, Inorg. Chem. 41 (2002) 1336.
[32] A. Puig-Molina, L. Pleth Nielsen, A.M. Molenbroek, K. Herbst, Catal. Lett. 92 (2004) 29.
[33] U. Riaz, O.J. Curnow, M.D. Curtis, J. Am. Chem. Soc. 116 (1994) 4357.
[34] S.H. Druker, M.D. Curtis, J. Am. Chem. Soc. 117 (1995) 6366.
[35] M.D. Curtis, J. Cluster Sci. 7 (1996) 247.
[36] M. Feliz, R. Llusar, S. Uriel, C. Vicent, M. Brorson, K. Herbst, Polyhedron 24 (2005) 1212.
[37] T. Tatsumi, M. Taniguchi, S. Yasuda, Y. Ishii, T. Murata, M. Hidai, Appl. Catal. A: Gen. 139 (1996) L5–L10.
[38] M. Taniguchi, D. Imamura, H. Ishige, Y. Ishii, T. Murata, M. Hidai, T. Tatsumi, J. Catal. 187 (1999) 139.
[39] V.P. Fedin, J. Czyzniewska, R. Prins, T. Weber, Appl. Catal. A: Gen. 213 (2001) 123.
[40] K. Herbst, B. Rink, L. Dahlenburg, M. Brorson, Organometallics 20 (2001) 3655.
[41] K. Herbst, M. Monari, M. Brorson, Inorg. Chem. 40 (2001) 2979.
[42] A. Müller, R. Jostes, W. Eltzner, C.-S. Nie, E. Diemann, H. Bögge, M. Zimmermann, M. Dartmann, U. Reinsch-Vogell, S. Che, S.J. Cyvin, B.N. Cyvin, Inorg. Chem. 24 (1985) 2872.
[43] C. Sourisseau, R. Cavagnat, M. Fouassier, S. Jobic, P. Deniard, R. Brec, R. Rouxel, J. Solid State Chem. 91 (1991) 153.
[44] D.J. Parker, J. Chem. Soc. Dalton Trans. (1974) 155.
[45] A. Müller, T. Weber, Appl. Catal. 77 (1991) 243.
[46] M. Houalla, D. Broderick, V.H.J. de Beer, B.C. Gates, H. Kwart, Am. Chem. Soc., Div. Petrol Chem. Prep. 22 (1977) 941.
[47] E. Payen, R. Hubaut, S. Kasztelan, O. Poulet, J. Grimblot, J. Catal. 147 (1994) 123.
[48] E.J.M. Hensen, P.J. Kooyman, Y. van der Meer, A.M. van der Kraan, V.H.J. de Beer, J.A.R. van Veen, R.A. van Santen, J. Catal. 199 (2001) 224.
[49] H. Topsøe, R. Candia, N.-Y. Topsøe, B.S. Clausen, Bull. Soc. Chim. Belg. 93 (1984) 783.
[50] J. Bachelier, M.J. Tilliette, J.C. Duchet, D. Cornet, J. Catal. 87 (1984) 292.
[51] J.V. Lauritsen, S. Helveg, E. Lægsgaard, I. Stensgaard, B.S. Clausen, H. Topsøe, F. Besenbacher, J. Catal. 197 (2001) 1.